

# 非牛頓流體中之電泳現象探討

## Electrophoresis of spherical colloid particles in non-Newtonian Fluid

計劃編號: NSC90-2214-E-002-030

執行期限: 90/08/01-91/07/31

主持人: 李克強 台灣大學化工系 教授

一、中文摘要(關鍵字: 電泳, 泳動度, 卡羅流體, 非牛頓流體, 假性光譜法)

本研究採用假性光譜法及牛頓-拉福生疊代法對球形膠體粒子在非牛頓卡羅流體中的電泳行為進行數值模擬及探討。具有剪力稀薄 (shear thinning) 性質的卡羅流體有很好的應用性, 故將傳統牛頓流體中電泳數值模擬拓展至此領域。主要討論的系統是單一球形膠體粒子在球形空洞中懸浮於卡羅流體中。基於低表面電位及弱外加電場的假設, 可適用線性化的 Poisson-Boltzmann equation 來描述系統的平衡電位。我們發現當流體參數  $n$  (幕次常數) 愈低,  $\lambda$  (鬆弛時間常數) 愈高, 也就是黏度稀薄效應愈明顯時, 粒子的電泳泳動度愈高, 而且此效應在高  $\kappa a$  的範圍內尤其明顯。且在低  $n$  值和高  $\kappa a$  處, 一個反向的渦流會被誘發在近外邊界處, 此導因於剪力稀薄性質。

**ABSTRACT**(Keywords: Electrophoresis, Carreau fluid, electrophoretic mobility, non-Newtonian fluid, pseudo-spectral method)

In this study, we take a fresh look on the electrophoretic behavior of a single spherical particle in a spherical cavity in Carreau fluid. The Carreau fluid, a non-Newtonian fluid with a shear-thinning property, has wide applications in industrial process. We change the value of the fluid model parameter  $n$  (the power law exponent) and  $\lambda$  (the relaxation time constant), where the model reduces to a Newtonian fluid when  $n \rightarrow 1$  and  $\lambda \rightarrow 0$ , and then discuss the effects of the shear thinning property on the mobility of the particle(s) and the related distribution of stream function, the shear rate, and the fluid viscosity.

Based on the assumption of low zeta potential and weak external applied electrical field, the linearization of the Poisson-Boltzmann equation describing the equilibrium potential is valid. And we use the pseudo-spectral method and the Newton-Raphson iteration process to numerically simulate the motion of colloidal particles in the Carreau fluid under electrophoresis at different  $\kappa a$  and discuss the behavior.

We conclude that under lower  $n$  and higher  $\lambda$ , thus the shear thinning property more obvious, higher mobility results and the effect is more apparent under high  $\kappa a$ . The effect of change in  $n$  is stronger than the effect in  $\lambda$ . Furthermore, in the contour plots which describe the distribution of stream function and the shear rate, we find that when  $\kappa a$  is high and  $n$  is low, a second vortex is induced in the outer portion of the space between the two boundaries at the right and the left sides of the particles. This phenomenon is due to the shear thinning property.

二、計劃緣由與目的

The surface properties of a charged entity are often estimated by an electrophoresis measurement. Its theoretical basis was founded by Smoluchoski,<sup>1</sup> who showed that the electrophoretic mobility of a particle  $\mu_E$ , defined by the ratio  $U/E$ ,  $U$  and  $E$  being respectively the magnitude of the electrophoretic velocity and the strength of the applied electric field, and its zeta potential  $\zeta$  are related by

$$\mu_E = \frac{\varepsilon_r \varepsilon_0 \zeta}{\eta} \quad (1)$$

where  $\varepsilon_r$  and  $\eta$  are respectively the relative permittivity and the viscosity of the liquid phase, and  $\varepsilon_0$  is the permittivity of a vacuum. Equation 1 provides a concise, yet clear quantitative description for the behavior of a charged entity in an applied electric field, and is widely used in various areas in practice. It should be pointed out, however, that its derivation was based on the assumptions of rigid, nonconductive entity at low surface potentials, weak applied electric field, thin double layer, negligible double layer polarization and boundary effect, and Newtonian fluid. Various attempts have been made to extend the original analysis of Smoluchoski by relaxing some of these assumptions. The electrophoretic phenomenon is described by the so-called electrokinetic equations, which include the governing equations for the flow, the concentration, and the electric fields. Since these equations are coupled and highly nonlinear, solving them analytically is almost impossible. This difficulty can be often circumvented by considering limiting cases such as simple geometry, very thin or very thick double layers, and low surface potentials.<sup>1-8</sup> In general, a numerical scheme needs to be adopted.<sup>9-12</sup> Adopting a shooting method, O'Brien and White<sup>9</sup> were able to derive the electrophoretic velocity of a sphere in an infinite fluid for the case of arbitrary double layer thickness and surface potential taking the effect double layer polarization into account. Lee et al.<sup>10-13</sup> discussed the electrophoretic phenomenon of a concentrated spherical dispersion and that of a sphere in a spherical cavity; a pseudo-spectral method was proposed in the numerical procedure. The results are applicable to arbitrary electrical potential and double layer thickness, mixed type boundary condition, and double layer polarization.

Although electrophoretic phenomenon has been studied extensively, almost all of the available results are for the case where the liquid phase is a Newtonian fluid, and the corresponding result for the case of non-Newtonian fluid is extremely limited. Presumably, this is mainly due

to the difficulties involved in solving the electrokinetic equations. Recent studies reveal that the effect of non-Newtonian fluid needs to be considered in problems, which are of both fundamental and practical significance. For example, the addition of polymer to a colloidal dispersion to improve its stability leads to a shear thinning behavior in the liquid phase.<sup>14</sup> Non-Newtonian behavior may also arise from the increase in the volume fraction of the dispersed phase.<sup>15</sup> The volume fraction of the slurry used in semiconductor processing, for instance, can easily exceed ten percent, and assuming Newtonian behavior is unrealistic in this case.

The constitutive equations for a generalized Newtonian fluid (GNF) can be expressed as<sup>16</sup>

$$\boldsymbol{\tau} = -\eta(\dot{\boldsymbol{\gamma}})\dot{\boldsymbol{\gamma}} \quad (2)$$

$$\dot{\boldsymbol{\gamma}} = \nabla \boldsymbol{v} + (\nabla \boldsymbol{v})^T \quad (3)$$

In these expressions,  $\boldsymbol{\tau}$ ,  $\dot{\boldsymbol{\gamma}}$ ,  $\eta$ , and  $\boldsymbol{v}$  are respectively the stress tensor, the rate of strain tensor, the apparent viscosity, and the velocity of the fluid,  $\nabla$  is the gradient operator, and the superscript  $T$  denotes matrix transpose. Note that if the apparent viscosity remains constant, eqs 2 and 3 reduce to the constituent equations for a Newtonian fluid. Shear thinning fluid is one of the most important fluids, which exhibit non-Newtonian behavior. Carreau<sup>16,17</sup> proposed the following three-parameter correlation relation, the so-called Carreau model, for the description of the behavior of a shear-thinning fluid:

$$\eta(\dot{\boldsymbol{\gamma}}) = \eta_0 [1 + (\lambda \dot{\boldsymbol{\gamma}})^\beta]^{(n-1)/\beta} \quad (4)$$

where  $\eta_0$  is the viscosity corresponding to the minimum shear force,  $\lambda$  is the relaxation time constant,  $n$  is the power-law exponent (since it describes the slope of  $(\eta - \eta_\infty)/(\eta_0 - \eta_\infty)$  in the power-law region), and  $\beta$  is a dimensionless parameter that describes the transition region between the zero-shear-rate region and the power-law region. According to Carreau model, the variation of viscosity as a function of shear rate can be divided into three regions: (a) For small shear rates, the viscosity is insensitive to the variation in the shear rate, the so-called zero-shear-rate viscosity region. (b) If shear rate exceeds a critical value, the viscosity increases monotonically with the shear rate, the so-called power-law fluid region. (c) If shear rate is large, the viscosity becomes insensitive to the variation in the shear rate again, the so-called infinite-shear-rate viscosity region. Yasuda et al.<sup>18</sup> proposed the following five-parameter Carreau-Yasuda model:

$$\eta(\dot{\boldsymbol{\gamma}}) = \eta_\infty + (\eta_0 - \eta_\infty) [1 + (\lambda \dot{\boldsymbol{\gamma}})^\beta]^{(n-1)/\beta} \quad (5)$$

where  $\eta_0$  and  $\eta_\infty$  are respectively the zero-shear-rate viscosity and infinite-shear-rate viscosity. These two parameters are roughly constant, and their effects are usually insignificant. This five-parameter model has sufficient flexibility to fit a wide variety of experimental  $\eta(\dot{\boldsymbol{\gamma}})$  curves. It has proven to be useful for numerical calculations. It has the merit that if either  $n \rightarrow 1$  or  $\lambda \rightarrow 0$ , it reduces to a Newtonian fluid, and it becomes a power law fluid if  $\lambda$  is sufficiently large. For many concentrated polymer solutions, good fit can be obtained by choosing  $\beta=2$  and  $\eta_\infty=0$ . In particular, it is capable of

describing the characteristics of the melts of many polymeric materials of industrial significance such as high-density polyethylene, low-density polyethylene, and polystyrene.

In the present study the electrophoretic behavior of a particle in a non-Newtonian fluid is analyzed. In particular, the boundary effect is taken into account by considering a sphere in a spherical cavity.

### 三、研究方法和成果

Referring to Figure 1, we consider the electrophoresis of a rigid, non-conductive sphere of radius  $a$  in a non-conductive spherical cavity of radius  $b$ . Let  $H=(a/b)$ , which measures the significance of the presence of the cavity. The particle is placed at the center of the cavity, and the space between sphere and cavity is filled with a Carreau (shear-thinning) fluid. The spherical coordinates  $(r, \theta, \varphi)$  are chosen with its origin located at the center of the cavity. An electric field  $\boldsymbol{E}$  is applied in the  $Z$ -direction, the particle moves with velocity  $\boldsymbol{U}$ , and the cavity remained fixed. Suppose that  $\boldsymbol{E}$  is weak and the polarization of the double layer surrounding the particle is negligible.

Suppose that the spatial variation in the electrical potential  $\phi$  can be described by the Poisson equation

$$\nabla^2 \phi = -\frac{\rho_e}{\varepsilon} \quad (6)$$

where  $\varepsilon$  is the permittivity of the liquid phase, and  $\rho_e$  is the space charge density, which can be expressed by

$$\rho_e = \sum_{j=1}^N z_j e n_j \quad (7)$$

where  $N$  is the number of ionic species,  $z_j$  and  $n_j$  are the valence and the number density of ionic species  $j$ , and  $e$  is the elementary charge.

Suppose that the liquid phase is incompressible and the flow field can be described by the Navier-Stokes equation in the creeping flow regime. Then

$$\nabla \cdot \boldsymbol{v} = 0 \quad (8)$$

$$\rho_f \frac{\partial \boldsymbol{v}}{\partial t} = -\nabla \cdot \boldsymbol{\tau} - \nabla p - \rho_e \nabla \phi \quad (9)$$

In these expressions  $p$  is the pressure,  $\boldsymbol{v}$  and  $\rho_f$  are respectively the velocity and the density of liquid phase. Note that a body force term,  $-\rho_e \nabla \phi$ , is included in the Navier-Stokes equation to take the effect of electric force into account. The stress tensor  $\boldsymbol{\tau}$  in eq 9 is described by eqs 2 and 3, and the viscosity  $\eta$  in eq 2 is described by the Carreau model, eq 5. If the system is at a steady state, then the left-hand side of eq 9 vanishes. For convenience, the electrical potential is expressed as the sum of the equilibrium potential (or the potential in the absence of the applied electric field),  $\phi_1$ , and a perturbed electrical potential which arises from the applied electric field,  $\phi_2$ . Suppose that the spatial variation in the concentration of ionic species follows the Boltzmann distribution. Then, we have

$$\nabla^2 \phi_1 = -\frac{\rho_1}{\varepsilon} = -\sum_{j=1}^N \frac{z_j e n_{j0}}{\varepsilon} \exp\left[-\frac{z_j e \phi_1}{k_B T}\right] \quad (10)$$

$$\nabla^2 \phi_2 = -\frac{\rho_2}{\varepsilon} = \left[ \begin{array}{l} \sum_{j=1}^N \frac{z_j e n_{j0}}{\varepsilon} \exp\left[-\frac{z_j e (\phi_1 + \phi_2)}{k_B T}\right] \\ - \sum_{j=1}^N \frac{z_j e n_{j0}}{\varepsilon} \exp\left[-\frac{z_j e \phi_1}{k_B T}\right] \end{array} \right] \quad (11)$$

$$\phi = \phi_1 + \phi_2 \quad (12)$$

$$\rho_e = \rho_1 + \rho_2 \quad (13)$$

$$n_j = n_{j0} \exp\left[-\frac{z_j e (\phi_1 + \phi_2)}{k_B T}\right] \quad (14)$$

where  $n_{j0}$  is bulk concentration of species  $j$ ,  $k_B$  is the Boltzmann's constant, and  $T$  is the absolute temperature.

The procedure of solving eqs 8 and 9 can be simplified by applying a stream function formulation to reduce the number of variables. Let  $\psi$  be the stream function of the flow field under consideration. Taking curl on both sides of eq 9, employing eq 8, and expressing the  $r$ - and the  $\theta$ -components of fluid velocity,  $v_r$  and  $v_\theta$ , respectively as  $v_r = -(1/r^2 \sin \theta)(\partial \psi / \partial \theta)$  and  $v_\theta = (1/r \sin \theta)(\partial \psi / \partial r)$ , the governing equation for the stream function  $\psi$  can be obtained.

$$\begin{aligned} & \eta E^4 \psi + \sin \theta \left[ \left( \frac{\partial \eta}{\partial r} \dot{\gamma}_{r\theta} + r \frac{\partial^2 \eta}{\partial r^2} \dot{\gamma}_{r\theta} + r \frac{\partial \eta}{\partial r} \frac{\partial \dot{\gamma}_{r\theta}}{\partial r} + \frac{\partial^2 \eta}{\partial r \partial \theta} \dot{\gamma}_{\theta\theta} + \frac{\partial \eta}{\partial \theta} \frac{\partial \dot{\gamma}_{\theta\theta}}{\partial r} \right) \right. \\ & - \left. \left( \frac{\partial^2 \eta}{\partial r \partial \theta} \dot{\gamma}_{rr} + \frac{\partial \eta}{\partial r} \frac{\partial \dot{\gamma}_{rr}}{\partial \theta} + \frac{1}{r} \frac{\partial^2 \eta}{\partial \theta^2} \dot{\gamma}_{r\theta} + \frac{1}{r} \frac{\partial \eta}{\partial \theta} \frac{\partial \dot{\gamma}_{r\theta}}{\partial \theta} \right) \right. \\ & + \frac{\partial \eta}{\partial r} \left( \frac{1}{\sin \theta} \frac{\partial^3 \psi}{\partial r^3} - \frac{\cot \theta}{r^2 \sin \theta} \frac{\partial^2 \psi}{\partial r \partial \theta} + \frac{1}{r^2 \sin \theta} \frac{\partial^3 \psi}{\partial r \partial \theta^2} - \frac{2}{r^3 \sin \theta} \frac{\partial^2 \psi}{\partial \theta^2} + \frac{2 \cot \theta}{r^3 \sin \theta} \frac{\partial \psi}{\partial \theta} \right) \\ & - \left. \frac{\partial \eta}{\partial \theta} \left( -\frac{1}{r^2 \sin \theta} \frac{\partial^3 \psi}{\partial r^2 \partial \theta} - \frac{1}{r^4 \sin \theta} \frac{\partial^3 \psi}{\partial \theta^3} - \frac{1}{r^4 \sin^3 \theta} \frac{\partial \psi}{\partial \theta} + \frac{\cot \theta}{r^4 \sin \theta} \frac{\partial^2 \psi}{\partial \theta^2} \right) \right] \\ & = -\left( \rho \frac{e z}{k T} \right) \frac{\partial \phi_1}{\partial r} \frac{\partial \phi_2}{\partial \theta} \sin \theta \quad (15) \end{aligned}$$

Note that since the apparent viscosity varies with the shear rate, eq 9 is nonlinear, and an iterative procedure is necessary.

The governing equations and the associated boundary conditions are solved numerically by adopting a pseudo-spectral method<sup>19</sup> based on Chebyshev polynomials. The physical domain described by the spherical coordinates is mapped onto a square computational domain  $[-1,1] \times [-1,1]$ . The discretization of the computational domain yields a set of nonlinear algebraic equations, which are solved iteratively by applying Newton-Raphson's method.

#### 四、結論與討論

Figure 3 shows the variation of the scaled mobility  $\mu_E$  as a function of double layer thickness  $\kappa a$  at various values of parameter  $n$  for the case  $\lambda U/a$  is small, those

for larger values of  $\lambda U/a$  are presented in Figures 4 and 5. The results for the case of Newtonian fluid ( $\lambda U/a = 0$ ) are also presented in these figures for comparison. Figures 2 through 4 reveal that for a fixed  $\kappa a$ ,  $\mu_E$  increases with the increase in  $\lambda U/a$ . According to eq 5, the larger the value of  $\lambda$  the more significant the effect of shear thinning, and, therefore, the greater the mobility. Figures 2 through 4 also indicates that for a fixed  $\lambda U/a$ , the difference between the mobility based on the present shear-thinning fluid and that based on the corresponding Newtonian fluid increases with the increase in  $\kappa a$  and with the decrease in  $n$ . The latter is because the smaller the value of  $n$  the more significant the effect of shear thinning, as suggested by eq 5. The former can be explained by the following. Since no-slip condition is assumed on particle surface the characteristic shear rate for the present electrophoretic phenomenon can be measured by  $U/(1/\kappa)$ ; the larger its value the greater the shear rate. Therefore, if the double layer is thick ( $1/\kappa$  is small), the characteristic shear rate is small, and the effect of shear thinning becomes insignificant.

The variation of scaled mobility  $\mu_E$  as a function of double layer thickness  $\kappa a$  at various  $\lambda U/a$  for the case  $n$  is large is presented in Figure 5, and those for smaller values of  $n$  are illustrated in Figures 6 and 7. Figure 5 reveals that both the mobility based on the present shear-thinning fluid and that based on the corresponding Newtonian fluid increase with  $\kappa a$ , and for a fixed  $\kappa a$ , the difference between them increases with  $n$ . These observations are consistent with the results shown in Figures 2 through 4. Figures 5 through 7 also suggest that the difference in the mobility based on the present shear-thinning fluid and that based on the corresponding Newtonian fluid increases with the decrease in the magnitude of  $n$ . This is expected since the smaller the  $n$  the more significant the effect of shear thinning.

Figures 2 through 7 reveal that appreciable variation in  $\mu_E$  occurs when  $\kappa a$  is greater than unity. This is because, by referring to eq 34, the effect of  $\kappa a$  on the mobility is of square nature. Therefore, if  $\kappa a$  is smaller than unity, its influence is limited. However, as  $\kappa a$  exceeds unity, its influence becomes significant apparently.

#### ACKNOWLEDGMENT

This work is supported by the National Science Council of the Republic of China.

#### 五、參考文獻

1. Smoluchowski, M. *Z. Phys. Chem.* 1918, 92, 129.
2. Huckel, E. *Phys. Z.* 1924, 25, 204.
3. Henry, D.C. *Proc. R. Soc. London, Ser. A* 1931, 133, 106.
4. Booth, F. *Proc. R. Soc. London Ser. A* 1950, 203, 514.
5. Levine, S.; Neale, G.H. *J. Colloid Interface Sci.* 1974, 47, 520.
6. Kozak, M.W.; Davis, E.J. *J. Colloid Interface Sci.* 1989, 127, 497.
7. Kozak, M.W.; Davis, E.J. *J. Colloid Interface Sci.* 1989, 129, 166.
8. Ohshima, H. *J. Colloid Interface Sci.* 1997, 188, 481.

9. O'Brien, R.W.; White L.R. *J. Chem. Soc., Faraday Trans. 2* **1978**, *74* 1607.
10. Lee, E.; Chu, J.W.; Hsu, J.P. *J. Colloid Interface Sci.* **1998**, *205*, 65.
11. Lee, E.; Chu, J.W.; Hsu, J.P. *J. Colloid Interface Sci.* **1998**, *209*, 240.
12. Lee, E.; Yen, F.Y.; Hsu, J.P. *Electrophoresis* **2000**, *21*, 475.
13. Hsu, J.P.; Lee, E.; Yen, F.Y. *J. Chem. Phys.* **2000**, *112*, 6404.
14. Hunter, R.J., *Foundations of Colloid Science*, Vol. I; Oxford University Press: Oxford, 1989.
15. Hunter R.J., *Foundations of Colloid Science*, Vol. II; Oxford University Press: Oxford, 1989.
16. Bird, R.B.; Armstrong, R.C.; Hassager, O., *Dynamics of Polymer Liquids*, Vol.I, *Fluid Mechanics*; Wiley: New York, 1987.
17. Carreau, P.J., PhD Thesis, University of Wisconsin, Madison, 1968.
18. Yasuda, K.; Armstrong, R.C.; Cohen, R.E. *Rheol. Acta*, **1981**, *20*, 163.
19. Canuto, C.; Hussaini, M.Y.; Quarteroni, A.; Zang, T.A., *Spectral Methods in Fluid Dynamics*; Springer-Verlag: New York, 1986.

六、圖表

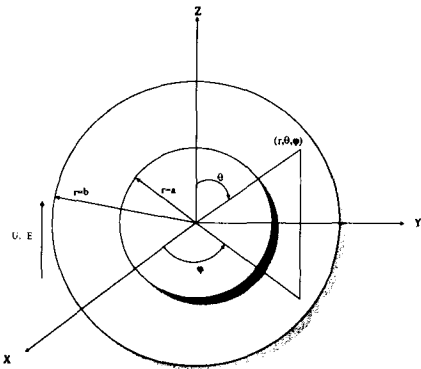


Fig.1. Geometric configuration of the cavity system in this study

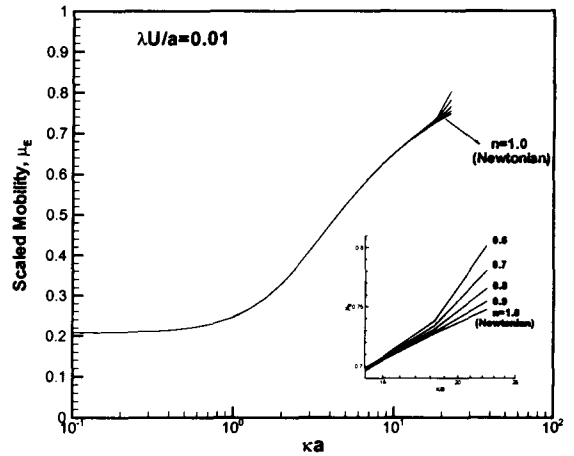


Fig.2. Variation of scaled mobility  $\mu_E$  as a function of double layer thickness  $ka$  at various values of parameter  $n$  for the case  $\lambda U/a = 0.01$ .

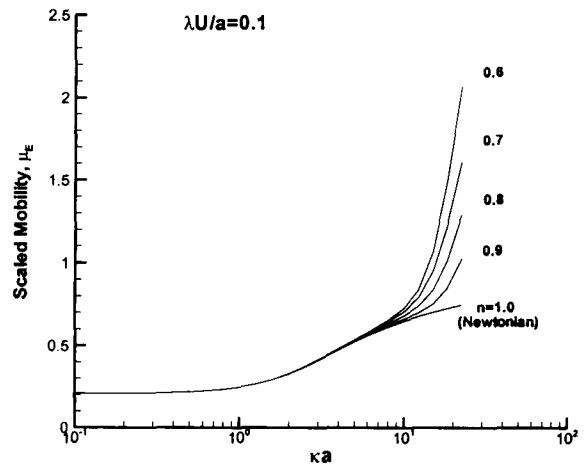


Fig.3. Variation of scaled mobility  $\mu_E$  as a function of double layer thickness  $ka$  at various values of parameter  $n$  for the case of Fig.5 except that  $\lambda U/a = 0.1$ .

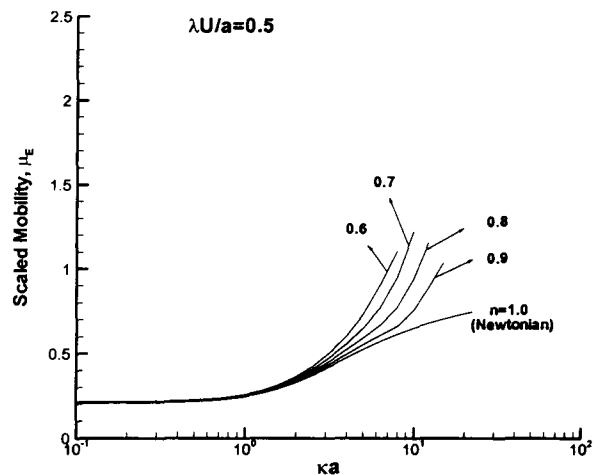


Fig.4. Variation of scaled mobility  $\mu_E$  as a function of double layer thickness  $ka$  at various values of parameter  $n$  for the case of Fig.5 except that  $\lambda U/a = 0.5$ .

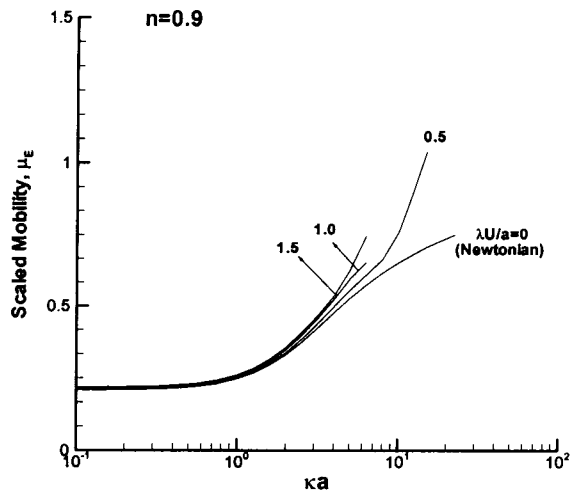


Fig.5. Variation of scaled mobility  $\mu_E$  as a function of double layer thickness  $\kappa a$  at various  $\lambda U/a$  for the case  $n=0.9$ .

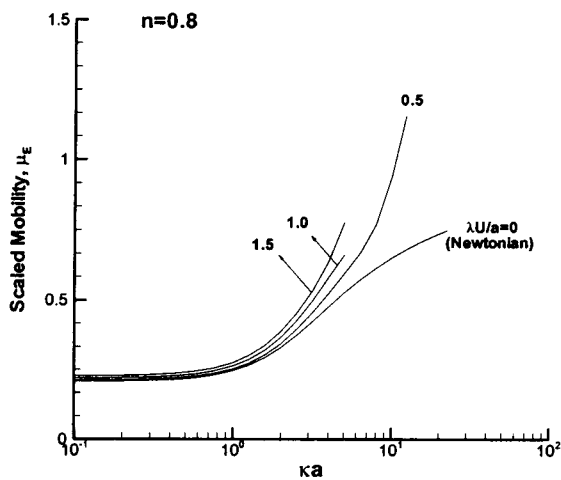


Fig.6. Variation of scaled mobility  $\mu_E$  as a function of double layer thickness  $\kappa a$  at various  $\lambda U/a$  for the case of Fig.2 except that  $n=0.8$ .

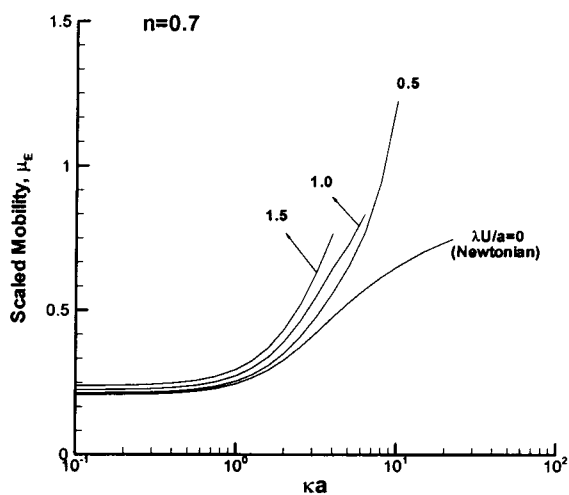


Fig.7. Variation of scaled mobility  $\mu_E$  as a function of double layer thickness  $\kappa a$  at various  $\lambda U/a$  for the case of Fig.2 except that  $n=0.7$ .